CFD Modeling of Varied Flow Conditions Over an Ogee-Weir

Gábor Fleit[1*], Sándor Baranya[1], Hans Bihs[2]

Abstract

Accurate estimation of discharge capacity and local hydrodynamics are essential when designing hydraulic structures. Instead of the application of conventionally used empirical relationships, this study introduces a 3D numerical modeling technique which is capable to adequately predict both the discharge-upstream water level relationship and the flow field around weirs. The numerical model, REEF3D, is validated for different hydrodynamic conditions (free-flow and submerged flow) against laboratory data performed for an ogee type weir. Simulated water surface elevations compared with experimental data together with the modeled flow field around the weir suggest that even the complex modular, transition and non-modular submerged cases can be reproduced by the numerical tool. The study proves that the herein applied numerical solver can be a good alternative of laboratory models for flow analysis at complex hydrodynamic conditions, especially where spatially strongly varying free surface characterizes the flow.

Keywords

CFD, weir, discharge coefficient, submerged flow

[1]Department of Hydraulic and Water Resources Engineering,
Faculty of Civil Engineering,
Budapest University of Technology and Economics,
H-1111 Budapest, P.O.B. 91, Hungary
[2]Department of Civil and Environmental Engineering,
Faculty of Engineering,
Norwegian University of Science and Technology,
7491 Trondheim, Norway
*Corresponding author, email: fleit.gabor@epito.bme.hu

1 Introduction

Weirs are very common structures in hydraulic engineering, usually used for water level control or other different purposes. In free-flowing conditions, when the tailwater has no influence on the upstream water level, critical flow is present above the crest by raising the channel bed and reducing the specific energy to a minimum. In these cases, there is a unique connection between the flow rate and the upstream water level (or pressure head), which can be exploited for flow measurements:

$$Q = C_f L H_u{}^a, \qquad (1)$$

where Q is the discharge, C_f is the free-flow discharge coefficient (not dimensionless), L is the width of the weir crest and H_u is the total upstream head (including the velocity head) measured from the crest of the weir, and the exponent a is typically equals 3/2. In order to design such structures for specific conditions, it is essential to get a good approximation of C_f as it determines the behavior of the weir during different hydrological events. Methods had been developed in the U.S., based on physical experiments to predict the value of C_f from the geometry of the structures, which indeed provide reasonable guidelines for engineers [1, 2]. However, if the tailwater level exceeds the level of the weir crest, submerged conditions appear where Eq. (1) is not valid anymore in the presented form, and C_f is to be replaced with the submerged discharge coefficient C_s.

Under submerged conditions, the upstream water level is influenced by the tailwater, hence here, Q is not only a function of H_u, but H_d (downstream total head measured from the top of the weir) as well and the level of submergence (S) can be written as:

$$S = \frac{H_d}{H_u}. \qquad (2)$$

Fig. 1 presents a sketch of an ogee weir, with the definition of total heads. It is noted that the heads should be measured/evaluated in a proper distance from the weir crest, both in the upstream and downstream directions in order to prevent problematic data connected to the highly turbulent, complex nature of the flow in the vicinity of the structure.

With S increasing, C_s becomes smaller and smaller, consequently the same discharge will result in higher upstream water levels compared to free-flow conditions, which may significantly increase flood risks upstream the weir. There are various semi-empirical methods available which take submergence into account [1, 3–5], however, laboratory experiments with an ogee-crested weir showed that these head-discharge relationships cannot provide reliable approximations, hence their applicability is to be questioned and further investigated [6, 7]. The experimental results discussed in [6, 7] give a thorough overview on the behavior of ogee-crested weirs under submerged conditions. The fact that the behavior of submerged weirs is basically determined by the geometry is duly noted, however, for the sake of simplicity only ogee type weirs will be concerned in the followings.
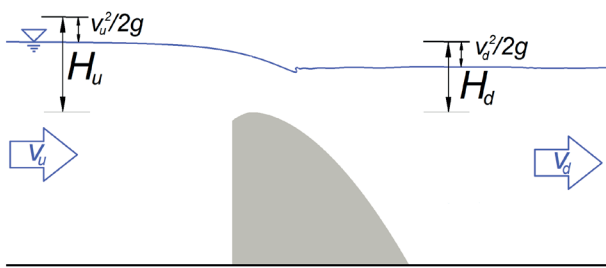

Fig. 1 Sketch of the ogee-crested weir, with the definition of the upstream and downstream total heads.

Based on the level of submergence, three main different flow conditions can be distinguished: modular, non-modular and the transition between these two. Despite in modular condition, the tailwater level exceeds the level of the weir crest, it only has minor effect on the head-discharge relationship, thus using the free-flow discharge coefficient is still a reasonable approach [8]. In such conditions, a submerged hydraulic jump appears right after the structure and the flow jet is attached to the downstream profile of the weir. In case of higher level of submergence, the hydraulic jump disappears, the jet detaches from the weir and a surface jet is formed, which results in the condition of non-modular flow. Within the transition, two subcategories may be further distinguished: at lower S values, the jet partly detaches from the weir profile with the submerged hydraulic jump persisting; while as getting closer to the non-modular condition, the surface jet evolves and a partial hydraulic jump still remains. According to [9] the transition between modular and non-modular conditions occurs in the $0.5 < S < 0.7$ range.

Based on the laboratory results presented by Tullis et al. [6, 7] Pedersen and Rüther conducted numerical experiments with the commercially available software Star-CCM+ to find out more about the mesh resolution dependency of a volume of fluids model for such cases [10]. Herein paper aims to present the numerical modeling of the same ogee-crested weir under various flow conditions in order to get a deeper understanding of the hydrodynamics of submergence and to show, that a

modern freely available computational fluid dynamics (CFD) software with a more adequate free surface capturing approach could also mean a potential candidate for solving such hydraulic engineering related flow problems.

2 CFD tool REEF3D

The numerical treatment of such complex flows (e.g. hydraulic jump) not only requires robust computational methods, but a proper free surface capturing as well. In order to provide these conditions, the open-source CFD tool REEF3D was employed to solve the fluid flow problem [11]. REEF3D has been successfully used for a wide range of hydraulic and marine engineering applications such as estimation of breaking wave forces [12], floating body dynamics [13], sediment transport [14] and wave run-up on river banks [15]. The code solves the incompressible, Reynolds-averaged Navier–Stokes (RANS) equations (Eq. (4)) together with the continuity equation (Eq. (3)) with finite difference method (FDM) which offers the straightforward implementation of high-order discretization schemes. The governing RANS equations, presented here in a Cartesian form, express the conservation of mass and momentum:

$$\frac{\partial U_j}{\partial x_j} = 0, \tag{3}$$

$$\frac{\partial U_i}{\partial t} + U_j \frac{\partial U_i}{\partial x_j} = -\frac{1}{\rho}\frac{\partial P}{\partial x_i} + \frac{\partial}{\partial x_j}\left(\left(v + v_t\right)\left(\frac{\partial U_i}{\partial x_j} + \frac{\partial U_j}{\partial x_i}\right)\right) + g_i, \tag{4}$$

where U is the velocity averaged over time t; x is the Cartesian spatial coordinate; ρ is the fluid density (considered constant here); P is the pressure; v is the kinematic viscosity; v_t is the turbulent eddy viscosity coming from the Boussinesq-approximation [16] and g is the acceleration due to gravity. Indexes i and j refer to Cartesian components of vector variables, and terms containing j are implicitly summed over $j = 1…3$.

The unknowns are discretized on a structured, orthogonal computational grid. The advective term is solved with the weighted essentially non-oscillatory (WENO) scheme [17] which results in accuracy of up to 5th-order and robust numerical stability, while temporal discretization is achieved with a 2nd-order total variation diminishing (TVD) Runge-Kutta scheme [18]. The pressure term is solved with the projection method [19] and the BiCGStab algorithm [20] with Jacobi scaling preconditioning. The RANS equations are closed with a two-equation k-ω model, which links turbulence to the Reynolds-averaged flow variables through the eddy viscosity concept [21]. The coefficients in these two additional partial differential equations had been set to their most commonly used values, according to [21].

As the flow problem that is to be investigated has a complex free surface, its proper treatment is essential in order to obtain accurate numerical approximations. The employed numerical tool REEF3D is a multiphase model, hence the governing

equations are not only solved for the water, but for the air phase as well. REEF3D employs the level set method (LSM) to capture the free surface between the phases [22], which promises a more precise and less grid resolution dependent solution for the position of the interface, compared to the widely used (e.g. in Star-CCM+, OpenFOAM, Flow-3D, ANSYS Fluent) VOF method [23]. The LSM uses a signed scalar function, called the level set function, to track the location of the free surface. The property of this function $\phi(\vec{x}, t)$, is that its value gives zero on the free surface, while in every other point of the domain it gives the closest distance to the interface and the phases are distinguished by the sign as follows:

$$\phi(\vec{x}, t) = \begin{cases} > 0, & if\ \vec{x} \in phase\ 1 \\ = 0, & if\ \vec{x} \in interface. \\ < 0, & if\ \vec{x} \in phase\ 2 \end{cases} \quad (5)$$

The interface then moves with the fluid flow and its movement can be described with the following advection equation:

$$\frac{\partial \phi}{\partial t} + U_j \frac{\partial \phi}{\partial x_j} = 0. \quad (6)$$

Structured, orthogonal grids are not very flexible, thus cannot be wrapped around complex geometries, which can easily become a problem when irregular structures are placed into the fluid domain or when working with natural topography. In order to overcome this problem, the ghost cell immersed boundary method (GCIBM) is used [24].

Full parallelization is achieved through the message passing interface (MPI) method. The computational domain is decomposed into n number of fractions, to each one is assigned a processor core. In order to maintain the continuity of the calculations, the boundaries of neighboring subdomains have to be shared, which is achieved through the employment of ghost cells [25].

3 Numerical setup
3.1 Computational domain
The numerical model was built up according to the experimental setup presented by [6, 7], in order to make the simulation results well comparable with the laboratory measurements. A 510.9 mm high ogee-crested weir was used in the experiments and its shape was designed with the compound curve method [1] with a design head (H_0) of 233.5 mm which accordin g to the given discharge coefficient C_f= 2.17 results in a specific design discharge (q_d) of 0.245 m²s⁻¹. Comparison of two-dimensional, width-averaged and three-dimensional numerical results for a similar ogee weir case showed, that due to the transversal symmetry of the geometry the flow conditions may also be considered 2D [26]. In order to preserve computational resources a 2D slice model was built up for the case. The numerical channel was built up from uniform hexahedron cells with side lengths of dx = 5 mm and had the following dimensions: 10.0 m long × 1.0 m high × 1 cell wide.

The evolving total heads were calculated using the time averaged water levels and the corresponding depth-averaged flow velocities. Total upstream heads were evaluated 2 m upstream from the crest, while downstream heads 5 m downstream of it. This ensured that the complex flow in the close vicinity of the structure does not affect the values which are to be directly compared with the experimental data.

The upstream face of the weir was located at 4.0 m from the upstream end of the flume to prevent numerical errors caused by the proximity of the inlet boundary.

3.2 Boundary conditions
The inlet boundary condition is prescribed as constant discharge which is distributed along the current water depth with the assumption of a logarithmic velocity profile. The RANS turbulence variables (turbulent kinetic energy (k) and specific turbulent dissipation (ω)) are distributed with a constant profile along the inflow boundary. The bottom of the channel and the weir geometry is treated as no-slip boundaries, while the two sidewalls as symmetry planes, i.e. a zero-gradient boundary condition is imposed on the pressure equation on the side boundaries. In absence of laboratory data regarding the roughness of the channel and the weir geometry, uniform effective roughness height k_s = 1.0 mm was set in the numerical model. Sensitivity analysis conducted to this parameter shown that the employment of different values in a realistic range (0.5–2.0 mm) does not result in notable deviation regarding the hydrodynamic solution. In terms of outflow boundaries, two significantly different types have to be distinguished: free outflow and controlled outflow. The free outflow boundary condition is applied for modeling free-flow conditions over the weir, where the tailwater does not affect the upstream head, which is achieved by allowing supercritical flow conditions downstream the structure. In case submerged conditions are to be investigated, controlled outflow boundary condition is applied, where the outflow water level is prescribed, i.e. a Dirichlet boundary condition is given.

4 Results
4.1 Free-flowing conditions
Depth control structures, such as ogee-weirs are usually designed for free-flowing conditions, when their capacity is not limited by the level of the tailwater, and the unique head-discharge relationship applies. The determination of this relationship – which is indeed very important from the operational aspect – is usually done with empirical formulas or in cases of high priority, through physical modeling. In this subsection, the verification of the numerical model will be presented through the simulation of free-flowing conditions to demonstrate the applicability of CFD and the herein employed tool in general in the solution of such engineering problems.

Numerical simulations had been conducted with seven different flow rates ranging from 40% to up to almost 150% of the specific design discharge, q_d and the resulting equilibrium upstream total heads (H_u) were compared with the experimental results (Table 1).

Table 1 Comparison of measured ($H_{u,meas}$) and simulated ($H_{u,sim}$) total upsteam heads for free-flowing conditions of different flow rates.

#	q [m²s⁻¹]	$H_{u,meas}$ [m]	$H_{u,sim}$ [m]	ΔH [m]	ΔH [%]
1	0.100	0.135	0.138	0.004	2.7
2	0.145	0.168	0.171	0.003	1.6
3	0.185	0.194	0.199	0.005	2.5
4	0.223	0.219	0.224	0.005	2.1
5	0.231	0.223	0.227	0.003	1.5
6	0.307	0.267	0.271	0.004	1.3
7	0.358	0.292	0.298	0.005	1.8

The model consequently overpredicts the upstream heads by 3 to 5 mm, which, in the presented discharge range, means a mean absolute percentage error (MAPE=$\sum_{k=1}^{n} \left| (M_i - S_i)/M_i \right| \cdot 100/n$, where M_i is the measured and S_i is the simulated value) of 1.96%. For actual engineering design purposes, this degree of inaccuracy is still considered reasonable, especially when these results are compared to the USBR prediction (coming from Eq. (1) with $C_f = 2.17$ for the herein presented geometry), which is, however, far faster and cheaper for present case than physical or even numerical modeling (Fig. 2).
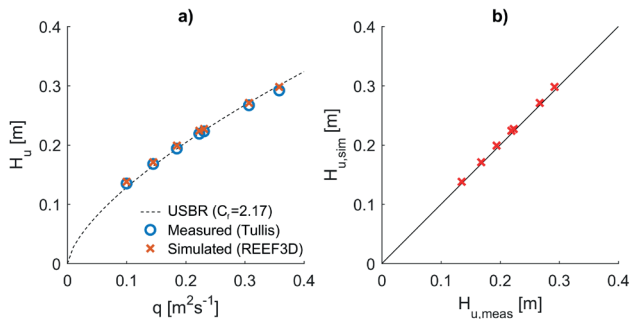

Fig. 2 a) Comparison of theoretical, measured and modeled head-discharge relationships; b) Comparison of modeled and measured upstream heads at different flow rates.

Slight deviations are observed between the theoretical and the measured values at Fig. 2a, which implies that the head-discharge relationship proposed by [1] works best at flow rates close to the design value, and gets worse as much lower/higher discharges occur. This is further supported by the fact, that the numerical model shows very similar behavior (compared to the measurements), however, the total upstream heads are numerically overpredicted.

4.2 Submerged scenario

If the downstream water level exceeds the level of the weir crest, submerged condition occurs. During such events, the regular head-discharge relationship cannot be applied as the capacity of the weir is limited by the tailwater. In this study, eleven numerical simulations had been conducted at design flow rate (Q_d) with different levels of submergence (ranging between approximately $S = 0.5...0.9$), which was achieved through using controlled outflow boundary conditions. Despite the employment of a Reynolds-averaged description, the highly turbulent nature of the evolving flow conditions resulted in velocity and free surface fluctuations, hence H_u (and from that S) was determined with further time averaging. The simulation results were compared with measured values in the same range of submergences (Fig. 3a).
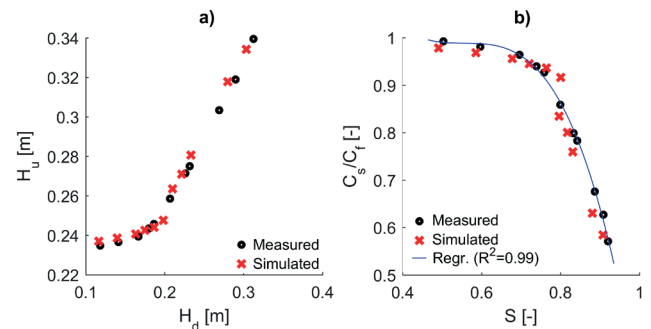

Fig. 3 a) Comparison of measured and modeled total upstream heads occurring due to different downstream total heads at design discharge; b) effect of submergence on the discharge coefficient (plotted as C_s/C_f).

The simulation results, in general, show good agreement with the experimental values in terms of the total head pairs (Fig. 3a), however, in most of the cases, slight overpredictions are again observed. In order to highlight the behavior of the weir and its relative capacity at different submergence levels, the ratio of the submerged and free-flowing discharge coefficients had been plotted as well, as a function of S (Fig. 3b). At $S \approx 0.8$ a small jump is observed in the model results, in contrast with the rather continuous curve suggested by the experimental data. Until this actual transition, the capacity reduction due to submergence is much milder and also changes in a lower rate with S (the steepness of the curve is smaller), while for $S > 0.8$, a much higher gradient is observed, the potential flow rate above the weir – represented through the discharge coefficient – responds badly to even smaller changes in the tailwater level. The nature of the experimental data can be well captured with a 3rd-order polynomial regression curve ($R^2 = 0.99$) as presented in Fig. 3b. Comparing the modeled data with the regression-curve an average error of –2.3% is present for the $S - C_s/C_f$ relationship, which means that in average, the model overestimates the capacity reducing effect of submergence, which is from the designing aspect a misprediction towards safety. The results not only underline the sensitivity of the model to this transition, but the sensitivity and complexity of the whole flow feature is highlighted as well.
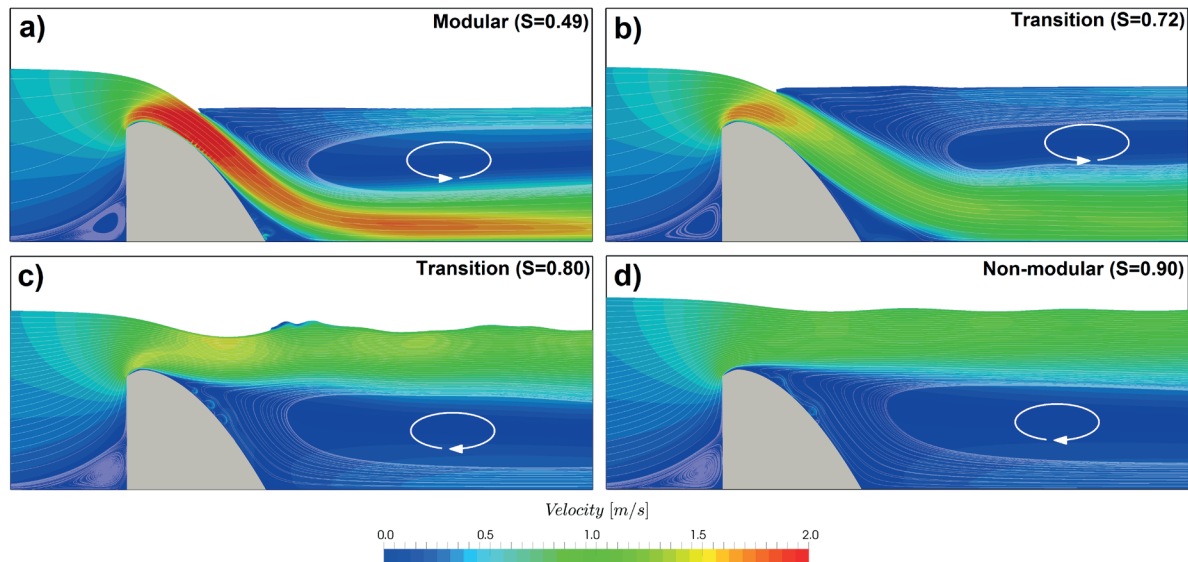
Fig. 4 Velocity contours with streamlines for the four different types of submerged flow conditions: a) modular flow with submerged hydraulic jump ($S = 0.49$); b) transition with detached jet and submerged hydraulic jump ($S = 0.72$); c) transition with surface jet and partial hydraulic jump ($S = 0.80$); d) non-modular flow with surface jet ($S = 0.90$).

In the introduction, it has been mentioned, that based on the level of the actual submergence, three different flow conditions can be distinguished: modular, non-modular and transition, and that the latter may be further divided into two subcategories. Fig. 4 is presented in order to provide a thorough overview of these flow conditions through velocity contour plots.

In the modular regime ($S < 0.7$), the tailwater level has only minor capacity reduction effect on the weir (Fig. 4a). The velocity field around the structure is rather similar to the free-flowing case as the jet is attached to the weir profile however, on the downstream side subcritical conditions occur. The shear zone at the upper edge of the jet results in robust counterclockwise recirculation in the upper two-third of the water column, where consequently no effective discharge transport is present. As a result, the high flow velocities persist after the overflow as well, forced to the bottom of the channel which means that for such scenarios, the apron has to be designed and constructed with special care, as strong erosion forces are expected.

As the downstream water level increases ($0.7 < S < 0.8$), the jet detaches from the weir and gradually tends towards the free surface (Fig. 4b). Maximal velocities on the downstream section are halved compared to the modular flow regime, consequently the recirculation zone is much thinner as well. Further increase of submergence pushes the jet to the surface with a partial hydraulic jump remaining (Fig. 4c). As the jet moves from the bottom to the surface, the location and the direction of the recirculation changes as well. In Fig. 4c it is observed, that the clockwise recirculation appears between the jet and the bottom of the channel, similarly to the non-modular case (Fig. 4d). Fully non-modular flow conditions occur when $S > 0.8$ (Fig. 4d). In these cases, the hydraulic jump completely disappears as the steady surface jet evolves with an orderly waved free surface profile. The recirculation does not change effectively compared to the one observed at Fig. 4c.

In overall, the numerical model adequately simulates the water surface elevations on both sides of the structure and the resulted discharge coefficients also show satisfactory agreement with laboratory data. The accurate estimation of these parameters inherently means the correct calculation of the flow field around the structure. The most significant disagreement with the measurements, which was still acceptable, was found at the transition flow conditions which indeed show reasonably complex character due to the wavy nature of the free surface, the recirculating and the jet like flow. A more detailed numerical model validation could be performed based on measured flow velocity and turbulence features, which might be a topic of future research.

5 Summary

The open-source CFD tool REEF3D has been presented and verified for the numerical modeling of varied flow conditions over an ogee-crested weir. The up-to-date numerical methods implemented in the FDM solver provide efficiency in solving the governing equations, while the high-order schemes ensure accurate and numerically stable spatial and temporal discretization. In contrast with the commercially available and widely used CFD models, which usually employ the Volume of Fluid method for the treatment of multiphase flows, the herein presented tool utilizes the Level Set Method, which is a more adequate tool for capturing the complex free surface in open-channel flow conditions.

The model verification was conducted through the evaluation of the head-discharge relationship for free-flowing scenarios over the weir, where the tailwater level does not affect the capacity of the structure. Simulation results were compared with results from laboratory experiment conducted by Tullis et al. [6, 7] and the total upstream heads were reproduced with a mean absolute percentage error of 1.96%.

After briefly overviewing the possible flow conditions during submergence, the numerical modeling of such events was conducted as well, as a main subject of the present paper. In order to highlight the response of the weir capacity to the level of submergence, S and C_s/C_f were plotted against each other (measured and simulated data as well) and the inaccuracy of the simulations were interpreted in the same sense as well. Calculations showed a MAPE of 3.94% and generally overpredicted the capacity reduction due to submergence, which from the designing aspect is a misprediction towards safety. The numerical model performed worst around S≈0.8, where the actual transition happens between diving jet to surface set, which is clearly rather challenging from the numerical modeling aspect.

The nature of the different flow conditions evolving during submerged conditions was presented through velocity contour plots, where streamlines also supported the apprehension of complex flow features. The LSM was indeed found to be a proper method for capturing the free surface, as even the evolving hydraulic jumps were stably reproduced in all cases.

6 Conclusions

The open-source CFD software REEF3D was found to be an adequate tool for the numerical modeling of free-flowing conditions over an ogee-crest weir as the simulated results showed good agreement with laboratory data. This means, that the head-discharge relationship and the free-flowing discharge coefficient in particular could be well approximated with such methods for any given geometry, even where standardized methods (such as in [1, 27]) are not available.

In terms of submerged conditions, where the level of the tailwater exceeds the weir crest, the available empirical formulas to take account for the capacity reduction due to submergence are inapt [6, 7], the effect is to be further investigated with experimental and numerical methods.

This study showed, that the computational treatment of such flow conditions is feasible with freely available, up-to-date CFD modeling tools, which clearly offers a considerable alternative compared to costly and time demanding physical modeling. The results also highlighted the sensitivity of CFD modeling for the present case: the transition from modular to non-modular conditions resulted in slightly higher disagreement compared to the less complex flow situations. Further spatial refinement of the computational mesh might be a way to increase the model robustness, however, considering the computational capacities available for the authors, simulations with much finer discretization would have required unreasonable simulation times.

Although, herein paper only dealt with the 2D modeling of a transversally symmetric weir, it is noted, that the code offers the opportunity to investigate weirs of more complex three-dimensional geometry, such as vee weirs or complete dam systems, where the resulting complex flow conditions e.g.

freefalling jets are also treatable owing to the LSM. Nevertheless, three-dimensional simulations with the herein presented spatial resolution does require serious computational resources and proper experimental data for verification.

Despite the fact that physical models are exempt from these sources of errors, they also have their own drawbacks, namely the scale effects [28]. In cases of high priority with the consideration of the previous weaknesses of the two modeling techniques, the best practice is the combined utilization of both investigation methods (e.g. [29]).

The highly turbulent nature of the presented flow conditions, also calls for the implementation of more advanced turbulence modeling techniques, such as Large Eddy Simulation (LES) [30]. In case there is an obstacle built in the water (e.g. bridge pier, weir, groin) which leads to a spatially strongly varying flow field, a RANS approach may result in inaccurate water level predictions around these structures, despite the numerical approximation of the velocity field is correct in general [31, 32].

It has to be underlined that in real hydraulic engineering problems, especially in the vicinity of hydraulic structures, one of the main issues to manage is related to the movement of sediments. Local scouring and local deposition of sediment generally occurs at obstacles in the flow which influence the stability of the structure. Consequently, beyond the approximated solution of the fluid flow problem, predictions toward potential morphological changes are also necessary when designing such structures. As a matter of fact, the presented numerical tool can be coupled with an extensive sediment transport module as well providing a suitable tool for morphodynamic simulations, based on which the scouring phenomenon and the rate of erosion in the close proximity of different obstacles might be revealed [14, 33]. Due to the complex nature of flow-sediment interactions and the significantly higher data demand of model validation, this paper could not deal with this problem, but the coupled hydrodynamic and sediment transport modeling shall be the topic of the next step in this research.

References

[1] USBR. *Design of small dams*. U.S. Depertment of Interior, Bureau of Reclamation. 1987. https://www.usbr.gov/tsc/techreferences/mands/mands-pdfs/SmallDams.pdf

[2] USACE. *Hydraulic design of spillways* (EM 1110-2-1603.). U.S. Army Corp of Engineers. 1990. http://www.publications.usace.army.mil/Portals/76/Publications/EngineerManuals/EM_1110-2-1603.pdf

[3] Cox, G. N. *"The submerged weir as a measuring device: a method for making accurate stream flow measurements that involve small loss of head"*. University of Wisconsin. 1928.

[4] Skogerboe, G. V, Hyatt, M. L., Austin, L. H. *Design and Calibration of Submerged Open Channel Flow Measurement Structures: Part 4 - Weirs*. Salt Lake City, Utah. 1967. http://digitalcommons.usu.edu/cgi/viewcontent.cgi?article=1079&context=water_rep

[5] Varshney, R. S., Mohanty, S. K. "Discharge relations for submerged weirs". *Indian Journal of Power & River Valley Development*, 23(7), pp. 225–228. 1973.

[6] Tullis, B. P., Neilson, J. "Performance of Submerged Ogee-Crest Weir Head-Discharge Relationships". *Journal of Hydraulic Engineering*, 134(4), pp. 486–491. 2008. https://doi.org/10.1061/(ASCE)0733-9429(2008)134:4(486)

[7] Tullis, B. P. "Behavior of Submerged Ogee Crest Weir Discharge Coefficients". *Journal of Irrigation and Drainage Engineering*. 137(10), pp. 677–681. 2011. https://doi.org/10.1061/(ASCE)IR.1943-4774.0000330

[8] Clemmens, A. J., Wahl, T. L., Bos, M. G., Replogle, J. A. *Water measurement with flumes and weirs* (Rep. No. 5.). Wageningen: International Institute for Land Reclamation and Improvement. 2001. http://www2.alterra.wur.nl/Internet/webdocs/ilri-publicaties/publicaties/Pub58/pub58-h1.0.pdf

[9] Collins, D. L. "Discharge computations at river control structures". *Journal of the Hydraulics Division*, 102(HY7), pp. 845–863. 1976.

[10] Pedersen, Ø., Rüther, N. "Numerical modeling of submerged flow over ogee-weirs". In *River Flow 2016*. (Constatinescu,G., Garcia, M., Hanes, D. (Eds.)). St. Louis, Mo., US. July 12-15, 2016.

[11] Bihs, H., Kamath, A., Alagan Chella, M., Aggarwal, A., Arntsen, Ø. A. "A new level set numerical wave tank with improved density interpolation for complex wave hydrodynamics". *Computers & Fluids*, 140, pp. 191–208. 2016. https://doi.org/10.1016/j.compfluid.2016.09.012

[12] Kamath, A., Alagan Chella, M., Bihs, H., Arntsen, Ø. A. "Breaking wave interaction with a vertical cylinder and the effect of breaker location". *Ocean Engineering*, 128, pp. 105–115. 2016. https://doi.org/10.1016/j.oceaneng.2016.10.025

[13] Bihs, H., Kamath, A. "A combined level set/ghost cell immersed boundary representation for floating body simulations". *International Journal for Numerical Methods in Fluids*, 83(12), pp. 905–916. 2017. https://doi.org/10.1002/fld.4333

[14] Ahmad, N., Bihs, H., Afzal, M. S., Arntsen, Ø. A. "Three-Dimensional Numerical Modeling of Local Scour Around a Non-Slender Cylinder Under Varying Wave Conditions". In: *36th IAHR World Congres*. Delft, The Netherlands. pp. 1–14. 2015.

[15] Fleit, G., Baranya, S., Rüther, N., Bihs, H., Krámer, T., Józsa, J. "Investigation of the Effects of Ship Induced Waves on the Littoral Zone with Field Measurements and CFD Modeling". *Water*, 8(7), pp. 300–321. 2016 https://doi.org/10.3390/w8070300

[16] Boussinesq, J. *"Essai sur la theorie des eaux courantes"*. Mémoires présentés par divers savants à l'Académie des Sciences de l'Institut National de France. XXIII(1), pp. 1–680. 1877.

[17] Liu, X-D., Osher, S., Chan, T. "Weighted Essentially Non-oscillatory Schemes". *Journal of Computational Physics*, 115(1), pp. 200–212. 1994. https://doi.org/10.1006/jcph.1994.1187

[18] Gottlieb, S., Shu, C.-W. "Total Variation Diminishing Runge-Kutta Schemes". *Mathematics of Computation*, 67(22198), pp. 73–85. 1998. https://doi.org/10.1090/S0025-5718-98-00913-2

[19] Chorin, A. J. "Numerical solution of the Navier-Stokes Equations". *Mathematics of Computation*, 22(107), pp. 745–762. 1968. http://s3.amazonaws.com/academia.edu.documents/9301421/chorin_1968.pdf?AWSAccessKeyId=AKIAIWOWYYGZ2Y53UL3A&Expires=1495440467&Signature=XCERRR69WHUlJbzG62deZlcOOkw%3D&response-content-disposition=inline%3B%20filename%3D-Numerical_solution_of_the_Navier-Stok

[20] van der Vorst, H. A. "Bi-CGSTAB: A Fast and Smoothly Converging Variant of Bi-CG for the Solution of Nonsymmetric Linear Systems". *SIAM Journal on Scientific and Statistical Computing*, 13(2), pp. 631–644. 1992. https://doi.org/10.1137/0913035

[21] Wilcox, D. C. *"Turbulence Modeling for CFD"*. La Canada, California, U.S.: DCW Industries Inc. 1998.

[22] Sussman, M., P. Smereka, Osher, S. "A level set approach for computing solutions to incompressible two-phase flow". *J. Comput. Phys.*, 114(1), pp. 146–159. 1994. https://doi.org/10.1006/jcph.1994.1155

[23] Hirt, C. W., Nichols, B. D. "Volume of Fluid (VOF) methods for the dynamics of free boundaries". *Journal of Computational Physics*, 39(1), pp. 201–225. 1981. https://doi.org/10.1016/0021-9991(81)90145-5

[24] Berthelsen, P. A., Faltinsen, O. M. "A local directional ghost cell approach for incompressible viscous flow problems with irregular boundaries". *Journal of Computational Physics*, 227(9), pp. 4354–4397. 2008. https://doi.org/10.1016/j.jcp.2007.12.022

[25] Kjolstad, F. B., Snir, M. "Ghost Cell Pattern". In: *Proceedings of the 2010 Workshop on Parallel Programming Patterns - ParaPLoP '10, 1*, pp. 1–9. 2010. https://doi.org/10.1145/1953611.1953615

[26] Savage, B. M., Johnson, M. C. "Flow over ogee spillway: Physical and numerical model case study". *Journal of Hydraulic Engineering*, 127(8), pp. 640–649. 2001. https://doi.org/10.1061/(ASCE)0733-9429(2001)127:8(640)

[27] USACE. *Hydraulic design of spillways* (EM 1110-2-). U.S. Army Corp of Engineers. 1990.

[28] Pfister, M., Chanson, H. "Scale Effects in Physical Hydraulic Engineering Models". *Journal of Hydraulic Research*, 50(2), pp. 244–246. 2012. https://doi.org/10.1080/00221686.2012.654671

[29] Pedersen, Ø., Rüther, N. "Hybrid Modeling of a Gauging Station Rating Curve". *Procedia Engineering*, 154, pp. 433–440. 2016. https://doi.org/10.1016/j.proeng.2016.07.535

[30] Smagorinsky, J. "General Circulation Experiments With the Primitive Equations". *Monthly Weather Review*, 91(3), pp. 99–164. 1963. https://doi.org/10.1175/1520-0493(1963)091%3C0099:GCEWTP%3E2.3.CO;2

[31] Lee, D., Nakagawa, H. "Inundation Flow considering Overflow due to Water Level Rise by River Structures". *Annuals of Disaster Prevention Research Institute, Kyoto University*. 53B, pp. 607-616. 2010. http://www.dpri.kyoto-u.ac.jp/nenpo/no53/ronbunB/a53b0p64.pdf

[32] Fleit, G. *Validation of a 3D Morphodynamic Model for Complex Flows*. MSc Thesis. Budapest University of Technology and Economics. 2016.

[33] Afzal, M. S., Bihs, H. S. *3D Numerical Modelling of Sediment Transport under Current and Waves*. MSc Thesis. Norwegian University of Science and Technology. 2013.